The substrate effect on the in-plane orientation of vertically well-aligned ZnO nanorods grown on ZnO buffer layers

2005 Nanotechnology 16 2882

(http://iopscience.iop.org/0957-4484/16/12/025)

INSTITUTE OF PHYSICS PUBLISHING NANOTECHNOLOGY
Nanotechnology **16** (2005) 2882–2886 doi:10.1088/0957-4484/16/12/025

The substrate effect on the in-plane orientation of vertically well-aligned ZnO nanorods grown on ZnO buffer layers

Hsin-Ming Cheng[1,2], Hsu-Cheng Hsu[1], Song Yang[1], Chun-Yi Wu[1], Yi-Chin Lee[1], Li-Jiaun Lin[2] and Wen-Feng Hsieh[1,3]

[1] Department of Photonics and Institute of Electro-Optical Engineering, National Chiao Tung University, 1001 Tahsueh Road, Hsinchu 30050, Taiwan, Republic of China
[2] Material Research Laboratories, Industrial Technology Research Institute, Hsinchu 310, Taiwan, Republic of China

E-mail: wfhsieh@mail.nctu.edu.tw

Received 11 July 2005, in final form 29 September 2005
Published 20 October 2005
Online at stacks.iop.org/Nano/16/2882

Abstract
Vertically well-aligned ZnO nanorods were synthesized without employing any metal catalysts on various substrates including glass, Si(111), 6H-SiC(0001) and sapphire (0001), which were pre-coated with *c*-oriented ZnO buffer layers, by simple physical vapour deposition. The alignments of the ZnO nanorods on the different substrates depend on the crystallographic alignments of the pre-coated ZnO buffer layers. The ZnO nanorods grown on glass and Si(111) are vertically aligned but randomly oriented in the in-plane direction. In contrast, the vertically aligned ZnO nanorods on 6H-SiC(0001) and sapphire (0001) show an in-plane alignment with azimuthally sixfold symmetry, which indicates the epitaxial relationship between ZnO and the substrate. Similarly, photoluminescence measurements show the distinct appearance of ZnO nanorods on different substrates. Besides the UV band, which was attributed to the recombination of free excitons near the band edge, defect-related visible emissions were also observed for the samples grown on both glass and Si(111) substrates. However, the ZnO nanorods exhibit only strong band edge emission peaks with no noticeable deep level emissions when grown on the 6H-SiC(0001) and sapphire (0001) substrates, which confirms the good crystalline and optical quality of the epitaxial ZnO nanorods.

1. Introduction

ZnO is an efficient material for photonic device use in the wavelength range of ultraviolet to blue, since it has a wide band gap energy of 3.37 eV and a large exciton binding energy of 60 meV at room temperature. It is expected that exciton as well as polariton lasers will be fabricated using ZnO-related materials and that they will supplant GaN-related materials in the near future, because exciton-stimulated emission and optically pumped laser action in high quality ZnO epitaxial films have been observed [1, 2] at room temperature. Due to the optical losses, including not only those due to nonradiative recombination centres but also those due to trapping of excitons, the high quality of ZnO becomes even more necessary in the excitonic lasing process.

Recently, one-dimensional (1D) ZnO nanostructures, such as nanowires and nanorods, have attracted considerable attention owing to their good crystal quality and unique photonic properties [3, 4]. ZnO nanowires and nanorods are also expected to play an important role, as crystal quality and photonic properties interconnect, as functional units in the fabrication of electronic, optoelectronic, electrochemical and electromechanical devices with nanoscale dimensions [4–19]. However, the synthesis of an array of well-aligned ZnO nanowires and nanorods is of great interest because it is a necessary step for realizing nanophotonic devices, which

[3] Author to whom any correspondence should be addressed.

include light-emitting diodes and laser diodes. Different methods have been reported for fabricating arrays of well-aligned 1D ZnO nanostructures that include vapour transport and condensation methods [3, 4], template methods [19, 20], metal–organic source vapour deposition methods [21, 22] and buffer layer pre-coating methods [23–26]. In our previous reports, the conductive ZnO buffer layer behaves as the active nucleus for the growth of ZnO nanorods on a Si substrate [23] and the patterned area for selective growth of ZnO nanorods on a sapphire substrate [26]. Accordingly, the buffer layer pre-coating method is a promising candidate for photonic device applications. In order to speed up the practical use of such ZnO nanorod arrays, studies on the growth behaviour of vertically well-aligned ZnO nanorods on various substrates for different applications seem more and more imperative.

In this paper, we report that vertical arrays of well-aligned ZnO nanorods were synthesized on various substrates including glass, Si(111), 6H-SiC(0001) and sapphire (0001), which were pre-coated with *c*-oriented ZnO buffer layers. We will discuss the in-plane orientation relationship between ZnO nanorods and buffer layers below. The photoluminescence (PL) properties of the nanorods were also comparatively investigated.

2. Experiments

The pre-coated substrates and ZnO nanorods were fabricated by the following procedure. First, the ZnO buffer layers were grown on glass, Si(111), 6H-SiC(0001) and *c*-plane sapphire, by the pulsed laser deposition (PLD) technique using a KrF excimer laser (wavelength of 248 nm and pulse duration of 25 ns) to ablate a ceramic ZnO target (99.999%) at 600 °C for 2 h and *in situ* annealing for 1 h at 700 °C under the pressure of 10^{-8} Torr. The thicknesses of the ZnO buffer layers were around 900 nm under rough control. Then the substrates were loaded 2 cm above an alumina boat containing 1 g zinc metal balls. The boat was put in the middle of the tube furnace. The furnace temperature was increased to 550 °C and high purity argon gas was then introduced at a flow rate of 500 sccm. When the growth process was complete, the tube furnace was cooled to room temperature in Ar-gas ambient and a grey–white coloured product was found over the substrates.

The morphologies of the as-synthesized products were characterized using a field emission scanning electron microscope (FESEM; JEOL-6500), which was equipped with an energy dispersive spectroscopy (EDS; Oxford) facility. The crystal structure of the nanorods was analysed using a transmission electron microscope (TEM; JEOL JEM-2000FX). High resolution x-ray diffraction (HRXRD) measurements were performed in a Bede D1 diffractometer equipped with an asymmetrically cut Si(220) monochromator and horizontal divergence slits with a width of 100 μm and a height of 2 mm, to select the Cu Kα1 radiation. The room temperature photoluminescence (RTPL) was obtained using a 20 mW He–Cd laser at the wavelength of 325 nm and the emission light was dispersed by a TRIAX-320 spectrometer and detected by a UV-sensitive photomultiplier tube.

3. Results and discussion

Parts (a)–(h) of figure 1 show typical top- and oblique-view SEM photographs of the vertically well-aligned ZnO nanorods, with lengths of several micrometres, fabricated on the various substrates. As shown, non-uniform, less well-aligned ZnO nanorods grow on glass (figures 1(a) and (b)), Si(111) (figures 1(c) and (d)) and 6H-SiC(0001) (figures 1(e) and (f)). In the case of sapphire (0001) (figures 1(g) and (h)) substrates, vertically well-aligned ZnO nanorods of uniform diameter and length were formed. An especially interesting feature of the ZnO nanorods is the relationship of the in-plane orientation which was discovered from top-view SEM photographs by fast Fourier transformation (FFT), as shown in the insets. The insets in figures 1(a) and (c) display blurred spots. These show that the ZnO nanorods on glass and Si(111) are randomly oriented in the in-plane direction. In contrast, the vertically aligned ZnO nanorods on 6H-SiC(0001) and sapphire (0001) show an in-plane alignment with sixfold symmetry, confirmed by the hexagonal starlike spots, as shown in the insets in figures 1(e) and (g). Moreover, figures 2(a) and (b) show the magnified top-view SEM images of the ZnO nanorods on the Si(111) and sapphire (0001) substrates, respectively. The photographs reveal more evidence that the nanorods have different in-plane orientations when grown on

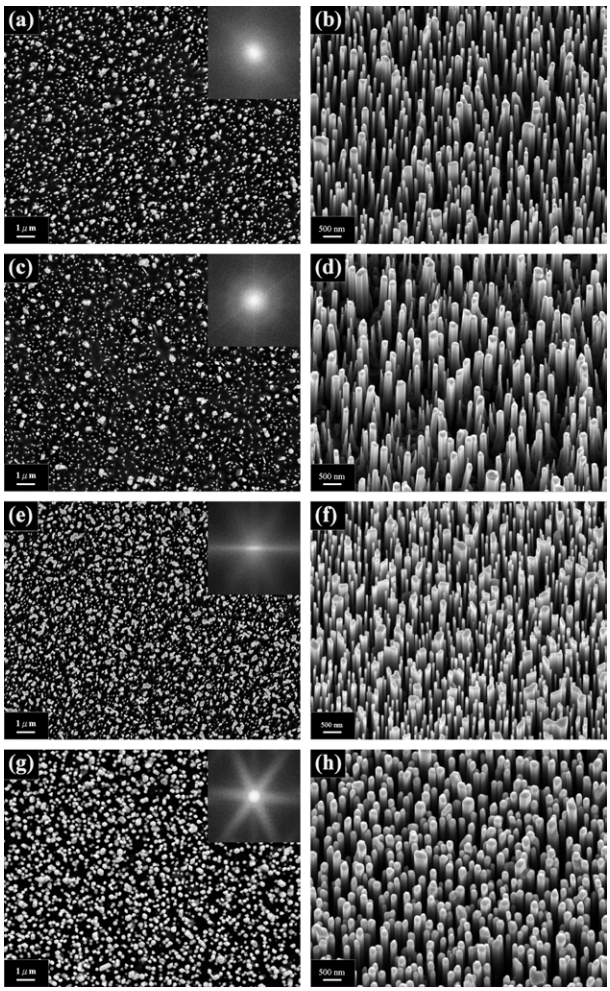

Figure 1. Top- and oblique-view SEM photographs of the vertically well-aligned ZnO nanorods fabricated on the various substrates: ((a), (b)) glass, ((c), (d)) Si(111), ((e), (f)) SiC(0001), ((g), (h)) sapphire (0001). The insets of (a), (c), (e) and (g) display the corresponding FFT images from top-view photographs.

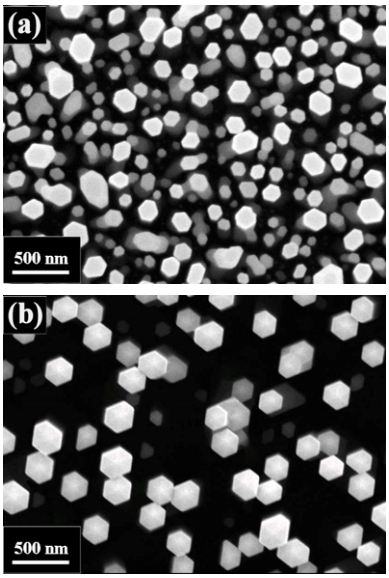

Figure 2. Magnified top-view SEM photographs of the vertically well-aligned ZnO nanorods fabricated on the (a) Si(111) and (b) sapphire (0001) substrates.

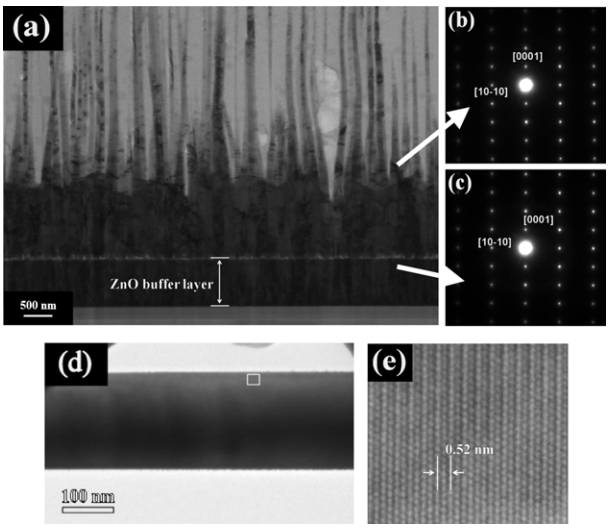

Figure 3. (a) Cross-sectional TEM image of ZnO nanorods grown on a ZnO buffer layer. ((b), (c)) SAED images of ZnO nanorods and the buffer layer, respectively. (d) Single-nanorod image; no catalyst particle at the end. (e) HRTEM image, showing the [0001] direction and the lattice spacing 0.52 nm.

different substrates. The sixfold facets of individual ZnO nanorods having the same direction shows the better epitaxial relationship for the rods on sapphire (0001) than on Si(111) and other substrates that we used. Since the ZnO nanorods were grown continuously above the pre-coated ZnO buffer layers, we firmly believe that the differences in relationships of in-plane orientations arise from the influences of the pre-coating layers.

Figure 3(a) shows a cross-sectional TEM image of ZnO nanorods on Si(111). The difference in brightness of the image is due to the diffraction from various crystallographic planes. Therefore, the ZnO film has a grainy and columnar structure. Furthermore, the ZnO nanorods were grown along

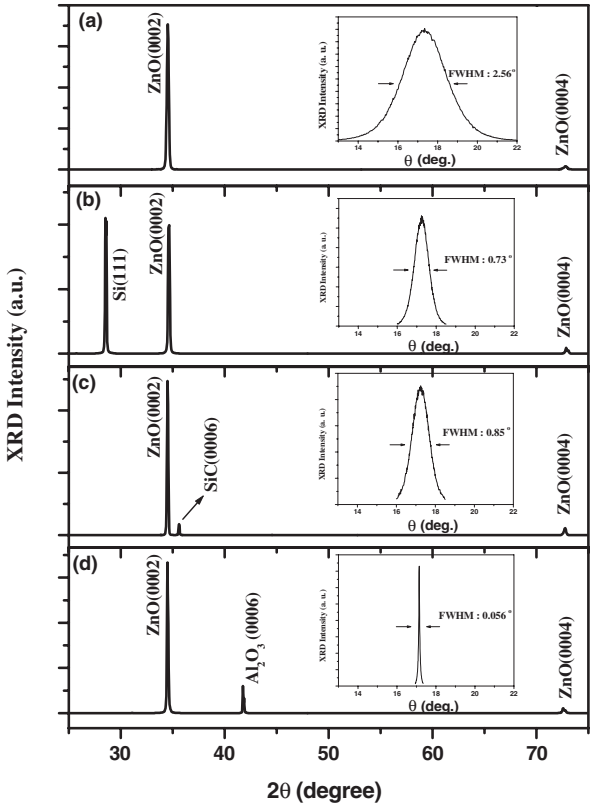

Figure 4. θ–2θ XRD profiles of ZnO nanorods on the various substrates: (a) glass, (b) Si(111), (c) SiC(0001), (d) sapphire (0001); and the corresponding ZnO(0002) θ rocking curves shown in the insets.

the columnar grains of the ZnO film. The ZnO buffer layer behaves as the active nucleus for the growth of ZnO nanorods. In addition, selected-area electron diffraction (SAED) patterns, as shown in figures 3(b) and (c), indicate that the columnar grains of the ZnO film were grown along the [0001] direction and hence the ZnO nanorods were also grown epitaxially along the same direction. Figure 3(e) shows a high resolution TEM (HRTEM) image confirming that the nanorods are single crystal and that the lattice spacing is approximately 5.2 Å along the *c*-axis, indicating again [0001] as the preferred growth direction for ZnO nanorods.

The ZnO buffer layer below governs the in-plane orientation of the ZnO nanorods above. Investigating the growth orientation and crystal alignment of the ZnO buffer layers grown on the substrates seems more significant. Various XRD techniques were performed. Figure 4 shows the θ–2θ x-ray diffraction patterns. Only the {0001} reflection family of ZnO and the surface parallel plane of the substrate appear in the wide angle XRD profile, indicating that all the ZnO films have a single ZnO phase as well as complete *c*-axis preferential growth. Meanwhile, the corresponding ZnO(0002) θ rocking curve was also obtained to investigate the degree of alignment with the normal of the surface, as depicted in the inset of figure 4. The ZnO buffer layer, which was grown on glass, shows a very broad vertical mosaic distribution of 2.56°, as shown in the inset of figure 4(a). The broad mosaic distribution causes some ZnO nanorods to grow at a slightly inclined angle, due to the mosaic grains behaving as a nucleus for growth of

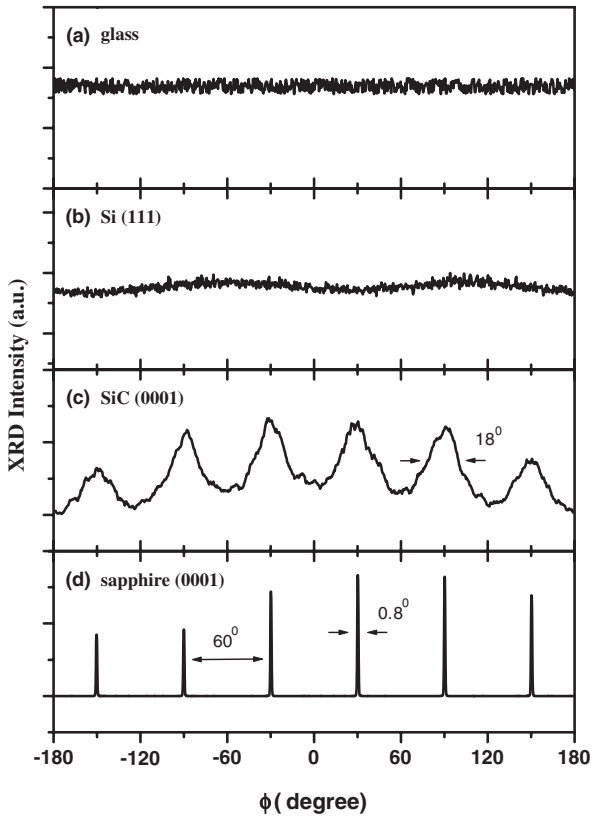

Figure 5. X-ray Φ-scan profiles of the ZnO($20\bar{2}2$) plane from ZnO nanorods on the various substrates: (a) glass, (b) Si(111), (c) SiC(0001) and (d) sapphire (0001).

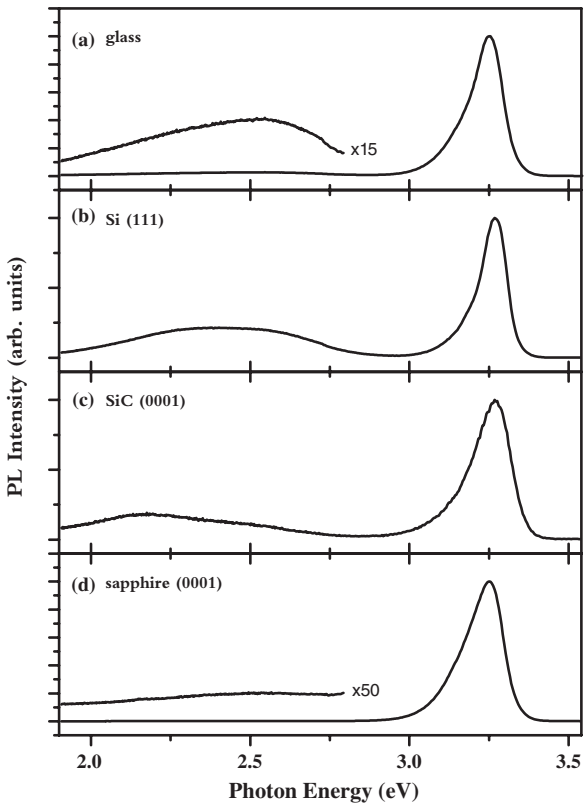

Figure 6. Typical room temperature photoluminescence (RTPL) spectra of ZnO nanorods on the various substrates: (a) glass, (b) Si(111), (c) SiC(0001) and (d) sapphire (0001). All the ZnO nanorods exhibit strong UV emission, and the distinct visible emissions, as shown enlarged in (a), (b) and (c), were attributed to nonstoichiometric defects.

ZnO nanorods. These features can be readily predicted since the glass substrate has an amorphous phase. Comparing with the glass substrate, the mosaic distributions become narrower: 0.73° and 0.85° for ZnO films grown on Si(111) and SiC(0001) substrates, respectively. Slightly tilted ZnO nanorods can also be found on those two substrates. It should be noted here that the mosaic distributions of the ZnO buffer layer on sapphire (0001) show extremely narrow FWHM values of 0.056°, as shown in the inset of figure 4(d), meaning that the buffer layers on the sapphire substrates were almost perfectly grown along the *c*-axial direction. Therefore, the ZnO nanorods reflect more uniformity and vertical alignment on sapphire (0001) compared to other substrates.

To explain the in-plane growth relationship of ZnO nanorods, XRD Φ-scan analysis of the ZnO($20\bar{2}2$) plane was used to investigate the ZnO buffer layers on different substrates. Figures 5(a) and (b) demonstrate that the ZnO buffer layers on glass and Si(111) have random alignment along the in-plane direction. The reasons are explained in terms of the amorphous phase for glass and the possible formation of an amorphous silica layer between ZnO and the Si substrate. Although the lattice mismatch between ZnO and Si(111) is ∼3.5%, the difficulty basically stems from the fact that the Si surface readily gets oxidized during the nucleation stage of a ZnO growth process [27]. In contrast, the ZnO buffer layers on 6H-SiC(0001) and sapphire (0001) exhibit an in-plane alignment with sixfold azimuthal symmetry, as shown in figures 5(c) and (d). Integrated evidence indicates that the epitaxial relationship between the ZnO buffer layer and 6H-SiC(0001) substrate would be $[0001]_{ZnO} \parallel [0001]_{SiC}$ along the normal to the substrate and $[10\bar{1}0]_{ZnO} \parallel [10\bar{1}0]_{SiC}$ along the in-plane direction. For the sapphire substrate the epitaxial relationship would be $[0001]_{ZnO} \parallel [0001]_{\alpha-Al_2O_3}$ and $[10\bar{1}0]_{ZnO} \parallel [11\bar{2}0]_{\alpha-Al_2O_3}$. In addition, the sharp peaks of the XRD Φ-scan for the ZnO buffer layer on sapphire (0001) indicate good alignment in the in-plane direction in comparison with the case for the buffer layer on SiC(0001). This result is also consistent with the FFT SEM image as shown by the sharp starlike spots when the ZnO nanorods were grown on sapphire (0001). Consequently, we consider that we have excellent normal and in-plane alignment for the ZnO buffer layer on sapphire (0001), therefore improving the growth of ZnO nanorods.

The RTPL spectra of the ZnO nanorods on different substrates are shown in figure 6. For all spectra, sharp ultraviolet (UV) peaks observed in the range of 3.0–3.4 eV were attributed to the exciton-related recombination. Furthermore, the weak green emissions in the range of 2.1–2.7 eV, attributed to the oxygen vacancies (V_O), are investigated when using glass and Si(111) substrates, as shown in figures 6(a) and (b). The weak yellow emission in the range of 1.9–2.4 eV, attributed to the oxygen interstitials (O_i), appeared when using the SiC(0001) substrate, as shown in figure 6(c). The strong UV emission with no visible band in the PL spectra indicates that the ZnO nanorods grown on sapphire

(0001) have a good crystal quality with few nonstoichiometric defects, as shown in figure 6(d). Various defect-related emissions were also reported in ZnO nanostructures fabricated by different methods [28]. In our work, we suppose the visible emissions to come from the interface between the pre-coated buffer layers and the nanorods, because of the strain and squeezing from discontinuous ZnO grains. Other analytical techniques such as cathodoluminescence will be used to resolve this controversy in our further investigations.

4. Conclusion

In summary, well-aligned ZnO nanorods were synthesized without employing any metal catalysts on glass, Si(111), 6H-SiC(0001) and sapphire (0001), which were pre-coated with *c*-oriented ZnO buffer layers. The alignments of the ZnO nanorods on the different substrates depend on the crystallographic alignment of the pre-coated ZnO buffer layer. Similarly, the photoluminescence measurements show the distinct appearance of ZnO nanorods on different substrates. Among those on the various substrates, ZnO nanorods grown on the sapphire (0001) substrate exhibit only a UV peak without noticeable visible emission, confirming epitaxial growth and good crystalline quality. Consequently, the crystal structure and characterization of the ZnO nanorods are basically related to the type of the substrate used.

Acknowledgments

The authors would like to gratefully acknowledge for financial support the National Science Council (NSC) in Taiwan under Contract No NSC-93-2112-M-009-035. We also thank the Nano Technology Research Centre (NTRC) for facility support and the TEM group of Material Research Laboratories (MRL) for help with electron microscopy measurements.

References

[1] Zu P, Tang Z K, Yu P, Wong G K L, Kawasaki M, Ohtomo A, Koinuma H and Segawa Y 1997 *Solid State Commun.* **103** 459
[2] Bagnall D M, Chen Y F, Zhu Z Q, Yao T, Koyama S, Shen M Y and Goto T 1997 *Appl. Phys. Lett.* **70** 2230
[3] Huang M H, Wu Y, Feick H, Tran N, Weber E and Yang P 2001 *Adv. Mater.* **13** 113
[4] Huang M H, Mao S, Feick H, Yan H, Wu Y, Kind H, Weber E, Russo R and Yang P 2001 *Science* **292** 1897
[5] Law M, Sirbuly D, Johnson J, Goldberger J, Saykally R and Yang P 2004 *Science* **305** 1269
[6] Johnson J C, Yan H Q, Yang P D and Saykally R J 2003 *J. Phys. Chem.* B **107** 8816
[7] Yan H, Justin J, Law M, Saykally R and Yang P 2003 *Adv. Mater.* **15** 1907
[8] Johnson J C, Knutsen K P, Yan H, Law M, Yang P and Saykally R 2004 *Nano Lett.* **4** 197
[9] Bai X D, Gao P X, Wang Z L and Wang E G 2003 *Appl. Phys. Lett.* **82** 4806
[10] Bai X D, Wang E G, Gao P X and Wang Z L 2003 *Nano Lett.* **3** 1147
[11] Kong X Y and Wang Z L 2003 *Nano Lett.* **3** 1625
[12] Arnold M, Avouris P, Pan Z W and Wang Z L 2003 *J. Phys. Chem.* B **107** 659
[13] Kong X Y, Ding Y, Yang R S and Wang Z L 2004 *Science* **303** 1348
[14] Kong X Y and Wang Z L 2004 *Appl. Phys. Lett.* **84** 975
[15] Hughes W L and Wang Z L 2004 *J. Am. Chem. Soc.* **126** 6703
[16] Zhao M H, Wang Z L and Mao S X 2004 *Nano Lett.* **4** 587
[17] Liu C H, Zapien J A, Yao Y, Meng X M, Lee C S, Fan S S, Lifshitz Y and Lee S T 2003 *Adv. Mater.* **15** 838
[18] Park W I and Yi G C 2004 *Adv. Mater.* **16** 87
[19] Park W I, Jun Y H, Jung S W and Yi G C 2003 *Appl. Phys. Lett.* **82** 964
[20] Zheng M J, Zhang L D, Li G H and Shen W Z 2002 *Chem. Phys. Lett.* **363** 123
[21] Park W I, Kim D H, Jung S-W and Yi G-C 2002 *Appl. Phys. Lett.* **80** 4232
[22] Wu J J and Liu S-C 2002 *Adv. Mater.* **14** 215
[23] Tseng Y K, Huang C J, Cheng H M, Lin I N, Liu K S and Chen I C 2003 *Adv. Funct. Mater.* **13** 811
[24] Tseng Y K, Chia C T, Tsay C Y, Lin L J, Cheng H M, Kwo C Y and Chen I C 2005 *J. Electrochem. Soc.* **152** G95
[25] Cheng H M, Hsu H C, Tseng Y K, Lin L J and Hsieh W F 2005 *J. Phys. Chem.* B **109** 8749
[26] Hsu H C, Tseng Y K, Cheng H M, Kuo J H and Hsieh W F 2004 *J. Cryst. Growth* **261** 520
[27] Nahhas A, Kim H K and Blachere J 2001 *Appl. Phys. Lett.* **78** 1511
[28] Li D, Leung Y H, Djurišić A B, Liu Z T, Xie M H, Shi S L, Xu S J and Chan W K 2004 *Appl. Phys. Lett.* **85** 1601